https://doi.org/10.46813/2023-148-180

# FORMATION AND PHENOMENOLOGICAL DESCRIPTION OF BREMSSTRAHLUNG BEAM FOR PHOTONUCLEAR PROCESSES

*V.L. Uvarov, A.A. Zakharchenko, N.P. Dikiy, Yu.V. Lyashko, R.I. Pomatsalyuk, V.A. Shevchenko, Eu.B. Malets**

*National Science Center "Kharkov Institute of Physics and Technology", Kharkiv, Ukraine;*
**H.S. Skovoroda Kharkiv National Pedagogical University, Kharkiv, Ukraine*
*E-mail: uvarov@kipt.kharkov.ua*

Within the framework of the developed analytical model for description of the isotope production by bremsstrahlung radiation, the three key phenomenological parameters of the process have been established. Those parameters determine the total yield and volumetric distribution of the products of a photonuclear reaction with dominating giant dipole resonance (GDR) in a target. The applicability conditions as well as the accuracy of the phenomenological description of a flux of the above-threshold bremsstrahlung photons are studied. The form of description of a reference bremsstrahlung spectrum for analytical calculation of the photonuclear processes is proposed. The conditions and accuracy of its reproduction at an electron accelerator are investigated.

PACS: 07.05.Tr, 41.50.+h; 41.75.Fr; 78.70.En

## INTRODUCTION

Photonuclear processes on the basis of the bremsstrahlung radiation are used to obtain a neutron beam with specified energy [1], to control a subcritical assembly [2], for transmutation of radioactive wastes [3], for photonuclear doping of semiconductors [4], in activation analysis of elemental and isotopic composition of matter [5], etc. In recent decades, the development of soft technologies for medical isotope production based on an electron accelerator has been actively carried out [6].

To calculate the photonuclear yield, a Monte Carlo simulation technique is commonly used. This technique requires a lot of computing time, especially when it is necessary to optimize a process with respect to a set of its parameters [7]. In [8], an analytical model (*S*-model) is presented for calculating the isotope generation in a target under the influence of bremsstrahlung radiation.

The aim of this study is to analyze the applicability boundaries and the accuracy of the proposed phenomenological description of the characteristics of a high-energy bremsstrahlung beam and of the photonuclear processes induced by it.

## 1. METHODS AND MATERIALS

### 1.1. A MODEL

1.1.1. A traditional scheme of a photonuclear process includes an intermediate target-converter made of a high- Z material placed at the exit of an electron accelerator to transform the electron beam into bremsstrahlung. An isotopic target is positioned on the radiation axes at a distance *a* from the converter.

In photonuclear technologies a thick converter is commonly applicated to increase the bremsstrahlung yield. In such a case the profile of the photon flux density is considered to be Gaussian [9]. For the effective utilization of the radiation, a target with width comparable to the width of the photon beam is applicated. As it is shown in [8], under such conditions the distribution of specific activity $\dot{A}$ of an isotope-product with decay constant $\lambda$ generated by an electron pencil beam with average current $I$ and energy $E_e$ at the end of the irradiation period $t$ can be represented in a rough approximation as:

$$\dot{A}(E_e,r,z)=Y_0(E_e)\frac{I\left[1-\exp(-\lambda t)\right]}{2\pi e\delta_\gamma^2(E_e,z)}\times$$
$$\times\exp\left\{-\left[\frac{r^2}{2\delta_\gamma^2(E_e,z)}+\mu(E_{\max})(z-a)\right]\right\}, \quad (1)$$

$$Y_0(E_e)=\frac{N_A}{\bar{A}}\nu\int_{E_{th}}^{E_e}n_\gamma(E,E_e)\sigma(E)dE, \quad (2)$$

$$\delta_\gamma(E_e,z)=\delta_{\gamma,0}(E_e)+z\cdot tg\theta_m(E_e). \quad (3)$$

where $N_A$ is the Avogadro's number; $\bar{A}$ is the average atomic weight of the target material; $\rho$ is its density; $\nu$ is the relative content of the target isotope; $\sigma(E)$ is the reaction cross section; $E_{th}$ is its threshold; $n_\gamma(E,E_e)$ is the photon spectrum integrated over the exit angle and normalized to one electron; $\delta_\gamma(E_e,z)$ is the standard deviation (SD) of the radial distribution of the above-threshold photon flux density at a distance $z$ from the rear surface of the converter; $\delta_{\gamma,0}(E_e)$ is SD of the radius of the photon escape from the converter; $\theta_m(E_e)$ is the most probable photon exit angle; $E_{max}$ is the photon energy corresponding to the GDR peak; $\mu(E_{max})$ is the linear attenuation coefficient for photons with energy $E_{max}$ in the target material.

As it can be seen from Eq.(1), the factor $Y_0(E_e)$ determines the overall activity of the target, while the values $\delta_\gamma(Ee,z)$ and $\theta_m(E_e)$ affect its volumetric distribution. Therefore, these three phenomenological parameters can be considered as the key characteristics of the process [8].

1.1.2. In a physical meaning $Y_0(E_e)$ corresponds to the reaction yield in a thin target normal to the photon beam axes and completely overlapping it, normalized to one primary electron and mass thickness of the target. The thickness of the latter should be much less than $\mu(E_{max})^{-1}$ – the free path of the photons with energy $E_{max}$ in the target material. By analogy with the bremsstrahlung converter, such a target was called a photonuclear converter (PNC), while $Y_0(E_e)$ was called the photonuclear conversion coefficient (CPC) – [8]. Its value can be determined in the experiment using the expression

$$Y_0^{\exp}(E_e) = \frac{eA_{PNC}(E_e,t)}{Id_{PNC}[1-\exp(-\lambda t)]}, \quad (4)$$

where $A_{PNC}(E_e,t)$ is the total activity of PNC at EOB, $d_{PNC}$ is its mass thickness. Thus to measure CPC it is necessary to estimate firstly the lateral dimension of the above-threshold photon flux in order to establish the minimum target width that meets the PNC conditions. The accuracy of the calculation of volumetric distribution of the induced target activity on the basis of the Eqs. (1)-(3) is determined by the accuracy of description of the reaction cross section $\sigma(E)$, the above-threshold photon spectrum integrated over the exit angle $n_\gamma(E,E_e)$, and also the standard deviation of their flux density $\delta_\gamma(E_e,z)$. In turn, the last parameter is determined by its value on the rear surface of the converter $\delta_{\gamma,0}(E_e)$ and the most probable exit angle of the above-threshold photons $\theta_m(E_e)$.

1.1.3. To measure SD of the flux density profile of the photons with energies higher than $E_{th}$ at a given distance $z$ from the converter, together with the PNC, a circular target of same material with size less than the width of the photon flux is aligned on the radiation axis providing a reaction with given threshold $E_{th}$. After irradiation of targets and measuring the activity of the radionuclide-product of the reaction, the SD value is determined using the expression

$$\delta_\gamma(E_e,z) = R_{ST}\left[-2\ln\left(1-\frac{A_{ST}(E_e,z)}{A_{PNC}(E_e)}\right)\right]^{-1/2}, \quad (5)$$

where $A_{ST}(E_e,z)$ is the activity of the small target, $R_{ST}$ is its radius. Thus to ensure the PNC irradiation mode, the width of the large target must exceed $6\delta_\gamma(E_e,z)$. To measure $\delta_{\gamma,0}(E_e)$, a pair of foils is placed directly on the rear surface of the converter.

The most probable exit angle of the bremsstrahlung photons can be measured by determination of SD of their flux profile at two points on the radiation axis with coordinates $z1$ and $z2$ using the expression

$$\theta_m(E_e) = \mathrm{arctg}\left(\frac{\delta_\gamma(E_e,z_2)-\delta_\gamma(E_e,z_1)}{z_2-z_1}\right), \quad (6)$$

or calculated by MC simulations with due regard to the characteristics of the primary electron beam, the accelerator exit window and the converter. The accuracy of the simulation results is about 6%.

1.1.4. In the framework of the *S*-model, a simple phenomenological formula has been proposed for the spectrum of high-energy bremsstrahlung photons integrated over the output angle and normalized to one primary electron, of form [8]

$$n_\gamma^S(E,E_e) = 2\eta(E_e)\left(E^{-1}-E_e^{-1}\right), \quad (7)$$

where $\eta(E_e)$ is the coefficient of energy conversion of electron into bremsstrahlung radiation. From this, one can obtain the expression for the total normalized-to-electron yield of the above-threshold photons

$$N_\gamma^S(E_{th},E_e) = 2\eta(E_e)\left[E_{th}\cdot E_e^{-1}-\ln\left(E_{th}\cdot E_e^{-1}\right)-1\right], \quad (8)$$

and also for the coefficient of transformation of electron beam energy into above-threshold photons

$$\eta(E_e,E_{th}) = \eta(E_e)\left(1-\frac{E_{th}}{E_e}\right)^2. \quad (9)$$

Considering the difficulty of the accurate measuring of the excitation function $\sigma(E)$ at the photon energy above 30 MeV [10], for a number of reactions the cross section averaged over the bremsstrahlung photon flux was studied (see, for example, [11]). Its value is determined by the expression

$$\langle\sigma(E_e)\rangle = \int_{E_{th}}^{E_e}\Phi_\gamma^T(E,E_e)\sigma(E)dE, \quad (10)$$

where the weighting function $\Phi_\gamma^T(E,E_e)$ is the energy distribution of the above-threshold photons on a target normalized to one photon. Within the framework of the *S*-model, for a target irradiated in the PNC mode with photon spectrum described by Eq. (7), one can obtain the explicit expression for the weighting function

$$\Phi_\gamma^S(E,E_e) = \frac{E^{-1}-E_e^{-1}}{E_{th}\cdot E_e^{-1}-\ln\left(E_{th}\cdot E_e^{-1}\right)-1}. \quad (11)$$

As it is evident from Eqs. (7)-(9) and (11), that the proposed description of the spectral characteristics of the above-threshold photons is unified, since it depends only on the boundaries $E_{th}$ and $E_e$ of the photon energy span. The conditions of the radiation formation (the converter material, its thickness, etc.) are taken into account through the energy conversion coefficient $\eta(E_e)$, which is included in the model expressions as a multiplier.

1.1.5. The accuracy of photon spectrum representation by the model was assessed by comparison with the results of the MC simulations. As a comparison parameter we considered the relative fraction of the above-threshold photons with energies up to 30 MeV (i.e., in the GDR region), which provides the main contribution to the flux-averaged cross section. In the general case, it is determined by the expression

$$\Delta(E_{th},E_e) = (N_\gamma(E_{th},E_e))^{-1}\int_{E_{th}}^{30MeV} n_\gamma(E,E_e)dE, \quad (12)$$

which in the *S*-model takes the form

$$\Delta^S(E_{th},E_e) = \frac{\ln\left(30\cdot E_{th}^{-1}\right)-(30-E_{th})E_e^{-1}}{E_{th}\cdot E_e^{-1}-\ln\left(E_{th}\cdot E_e^{-1}\right)-1}, \quad (13)$$

where $E_{th}$ and $E_e$ are given in MeV.

### 1.2. SIMULATIONS

The obtained experimental data and the predictions of the analytical model were compared with the results of the Monte Carlo simulations. A GEANT4.11 code [12] was used to calculate the characteristics of the bremsstrahlung photon flux at the converter output. The photon spectrum calculations were based on a G4EmPenelopePhysics model. The testing computations of the energy conversion coefficient $\eta(E_e)$ on the basis of the models G4EmLivermorePhysics and G4EmStandardPhysics_option4 have shown that the relative difference between the obtained data is no more than ±0.5%. This is less than the statistical uncertainty of the simulation results, which was ±1%.

### 1.3. EXPERIMENT

The experimental studies were carried out at a LUE-40 accelerator of NSC KIPT [13], which provides the electron beam energy in the range of 35…95 MeV at an average beam current of about 4 μA.

During the study of spatial characteristics of the bremsstrahlung beam, the two types of the exit window of the accelerator were used:

a single Ti foil by 50 μm in thickness ("thin" window);

the two Ti foils each 50 μm thick separated by a 3 mm gap for cooling water ("thick" window).

To obtain bremsstrahlung radiation, a converter comprising four tantalum plates each by 1 mm in thickness separated with the same air gaps was applied. The converter was positioned on the electron beam axis at a distance of 11 cm from the accelerator window.

To measure SD of the flux density profile of the above-threshold photons, the stacked pairs of foils from natural titanium by 50 μm in thickness and with diameter of 25 mm (PNC) and 6 mm (small target, ST) were used. After irradiation for about 1 h and cooling for a day, the activity of $^{47}Sc$ and $^{48}Sc$ isotopes in the foils with a HPGe γ-spectrometer was measured. The main channels of their generation are the reactions $^{48}Ti(\gamma,p)^{47}Sc$ and $^{49}Ti(\gamma,p)^{48}Sc$ with same threshold of 11.4 MeV. The $^{47}Sc$ yield was determined at the line 159.4 keV (68% branching ratio). The activity of $^{48}Sc$ was measured at the lines 983.5 keV (100%), 1037 (97.5%) and 1312 keV (100%). The total uncertainty of measurement of the $^{47}Sc$ activity was 9% and of $^{48}Sc$ – 4%. Comparison of results obtained for the both channels enables to assess their accuracy.

It should be noted the considerable scatter of data on the cross sections of those reactions presented in the literature [14-16]. At the same time, it does not affect the accuracy of a measurement of the photon beam width as it is determined by the ratio $A_{ST}/A_{PNC}$ of the activities of the foils.

## 2. RESULTS AND DISCUSSION

### 2.1. SPATIAL CHARACTERISTICS OF BREMSSTRAHLUNG BEAM

2.1.1. The performed analysis has shown that in the case of a narrow electron beam incident on the converter, the bremsstrahlung profile at its output is a combination of Lorentzian and Gaussian (Fig. 1,a). As the electron beam width increases, the weight fraction of the former decreases, while of the latter increases (Fig. 1,b).

By the MC simulations and with the use of a COD criterion, the estimates were obtained for the minimum SD of the electron flux density distribution on the converter $\delta_{e,gauss}$ as a conditional threshold for the Gaussian description of the photon beam profile (Table 1).

***Table 1***

*Minimum SD of the electron flux density to obtain Gaussian profile of the bremsstrahlung photon beam*

| $E_e$, MeV | $\delta_{e,gauss}$ , mm | Gaussian fitting COD |
|---|---|---|
| 40 | 1.07 | 0.9977 |
| 50 | 0.85 | 0.9964 |
| 60 | 0.75 | 0.9965 |
| 95 | 0.64 | 0.9983 |

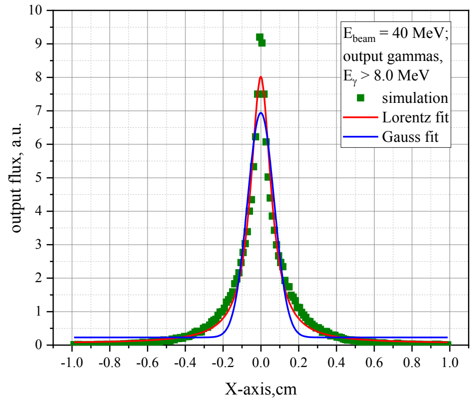


*a*

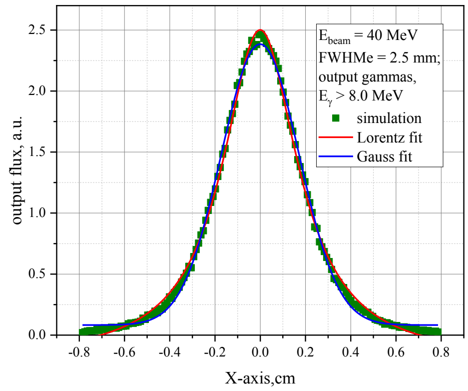


*b*

*Fig. 1. Profile of the above-threshold photon flux density (W converter 4 mm thick, $E_e$ = 40 MeV, $E_{th}$ = 8 MeV): a – $FWHM_e \approx 0$; b – $FWHM_e$ = 2.5 mm*

2.1.2. Under real conditions, an electron beam obtained in the vacuum chamber of an accelerator with SD of the flux density $\delta_{beam}$ is output through the exit window and travels some distance in air before interacting with the bremsstrahlung converter. Taking into account the scattering of electrons in those media, the expression for SD of the electron beam at the converter, $\delta_e$, can be represented in quadratures

$$\delta_e = \left(\delta_{beam}^2 + \delta_{e,\min}^2\right)^{1/2}, \tag{14}$$

where $\delta_{e,min}$ is SD of the electron flux density at the converter at $\delta_{beam} \approx 0$. In the case of $\delta_e > \delta_{e,gauss}$, one can determine SD of the photon flux density at the converter output by the expression

$$\delta_{\gamma,0} = \left(\delta_{beam}^2 + \delta_{\gamma,\min}^2\right)^{1/2}, \tag{15}$$

where $\delta_{\gamma,min}$ is SD of the photon flux density at $\delta_{beam} \approx 0$. It can be seen that in the case of $\delta_{beam} > \delta_{\gamma,min}$, the dependence $\delta_{\gamma,0}(\delta_e)$ can be fitted by a linear approximation (Fig. 2).

It turned out that for almost any width of the primary electron beam, the photon flux has a Gaussian shape. This is due to the scattering of electrons in the outlet window of the accelerator as well as in the air layer between it and the converter. It should be noted that the values of $\delta_e$ and $\delta_{\gamma,0}$ obtained by MC simulations are 1…3% higher than those calculated using Eqs. (14) and (15), as the latters do not consider the angular divergence of the electron flux incident on the converter. At $E_{th}$ in the range of 7…12 MeV, which is typical for one-nucleon reactions [5], the $\delta_{\gamma,0}$ values are differed by no more than 1.5%.

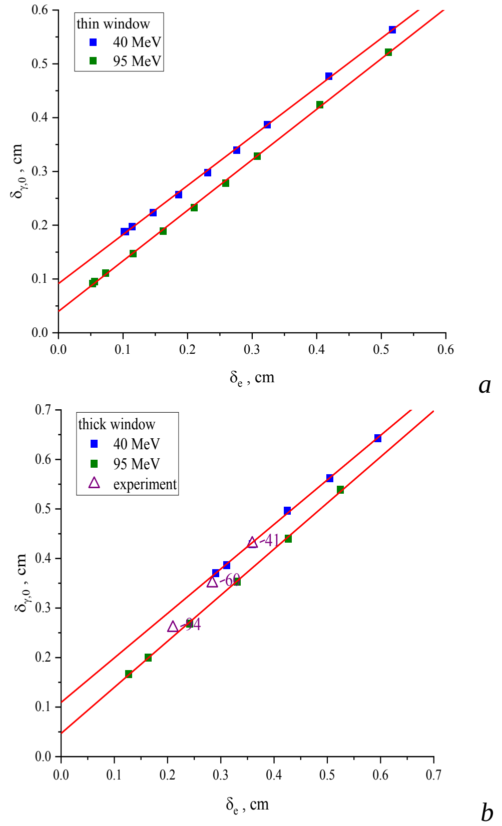


*Fig. 2. Linear approximation of dependence of the above-threshold photon flux density SD on SD of the electron flux density at the input of the converter (points correspond to the values obtained by MC simulations, figures at triangles show beam energy)*

***Table 2***

*The most probable exit angle of above-threshold photons (degree)*

| $E_e$, MeV | $d_c$, mm | | | | |
|---|---|---|---|---|---|
| | 1 | 2 | 3 | 4 | 5 |
| 40 | 4.6 | 5.6 | 6.2 | 6.4 | 6.5 |
| 60 | 3.4 | 4.1 | 4.7 | 5.1 | 5.3 |
| 80 | 2.7 | 3.5 | 3.9 | 4.2 | 4.3 |
| 95 | 2.5 | 3.1 | 3.4 | 3.7 | 3.9 |

Table 2 presents the results of the MC simulations of most probable angle of the photon escape from a W converter depending on its thickness $d_c$. Calculations have shown also its weak dependence on the reaction threshold in the range 7…12 MeV.

## 2.2. ABOVE-THRESHOLD PHOTONS SPECTRUM

Fig. 3 shows the dependence of the energy conversion coefficient $\eta$ on the thickness of the converter made of tungsten and tantalum. It can be seen that for both materials in the electron beam energy range of 40…95 MeV, the obtained curves behave in a similar way. The converter thickness of 4 mm is close to optimal. This conclusion is also confirmed by the results of the calculation of coefficient of electron radiation energy conversion into the above-threshold photons [8].

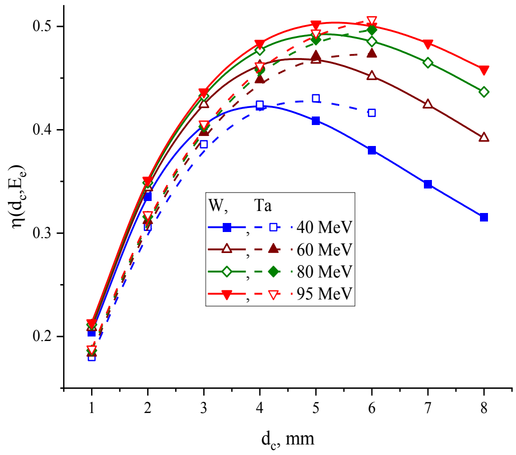


*Fig. 3. Energy conversion coefficient of electron into bremsstrahlung radiation (empty symbols – Ta, filled symbols – W)*

Table 3 presents the results of calculating the comparison parameter Δ for the spectra of bremsstrahlung photons with lower boundary of 7 and 12 MeV, obtained by Eq. (13), as well as by the MC simulations based on Eq. (12). It can be seen that at a W converter thickness of 3…4 mm, Eq. (7) describes most accurately the spectrum with deviation from the MC calculated values by no more than ±2%. Figs. 4 and 5 present the above-threshold photon spectra for a 4 mm W converter, normalized to one primary electron and one photon, respectively.

***Table 3***

*Relative fraction of photons within the GDR region (W converter)*

| $E_{th}$, MeV | $E_e$, MeV | S-model, Eq. (13) | *Monte Carlo simulations* | | | | | |
|---|---|---|---|---|---|---|---|---|
| | | | 1 mm | 2 mm | 3 mm | 4 mm | 5 mm | 6 mm |
| 7 | 40 | 0.959 | 0.918 | 0.940 | 0.952 | 0.958 | 0.960 | 0.961 |
| 7 | 60 | 0.847 | 0.782 | 0.816 | 0.844 | 0.865 | 0.879 | 0.889 |
| 7 | 80 | 0.766 | 0.705 | 0.740 | 0.772 | 0.798 | 0.820 | 0.836 |
| 7 | 95 | 0.721 | 0.664 | 0.700 | 0.733 | 0.762 | 0.787 | 0.806 |
| 12 | 40 | 0.925 | 0.866 | 0.899 | 0.916 | 0.924 | 0.927 | 0.929 |
| 12 | 60 | 0.761 | 0.677 | 0.717 | 0.750 | 0.775 | 0.792 | 0.804 |
| 12 | 80 | 0.660 | 0.586 | 0.623 | 0.657 | 0.686 | 0.710 | 0.728 |
| 12 | 95 | 0.608 | 0.542 | 0.577 | 0.611 | 0.642 | 0.667 | 0.689 |

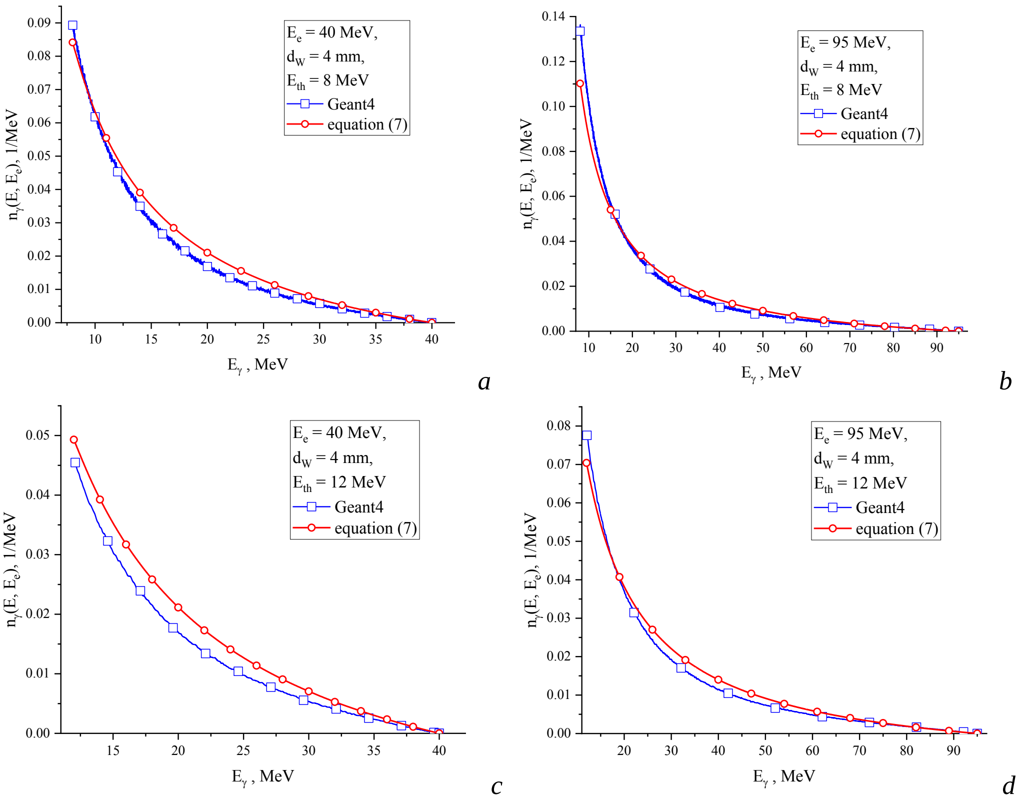


*Fig. 4. Above-threshold photon spectra normalized to one electron*

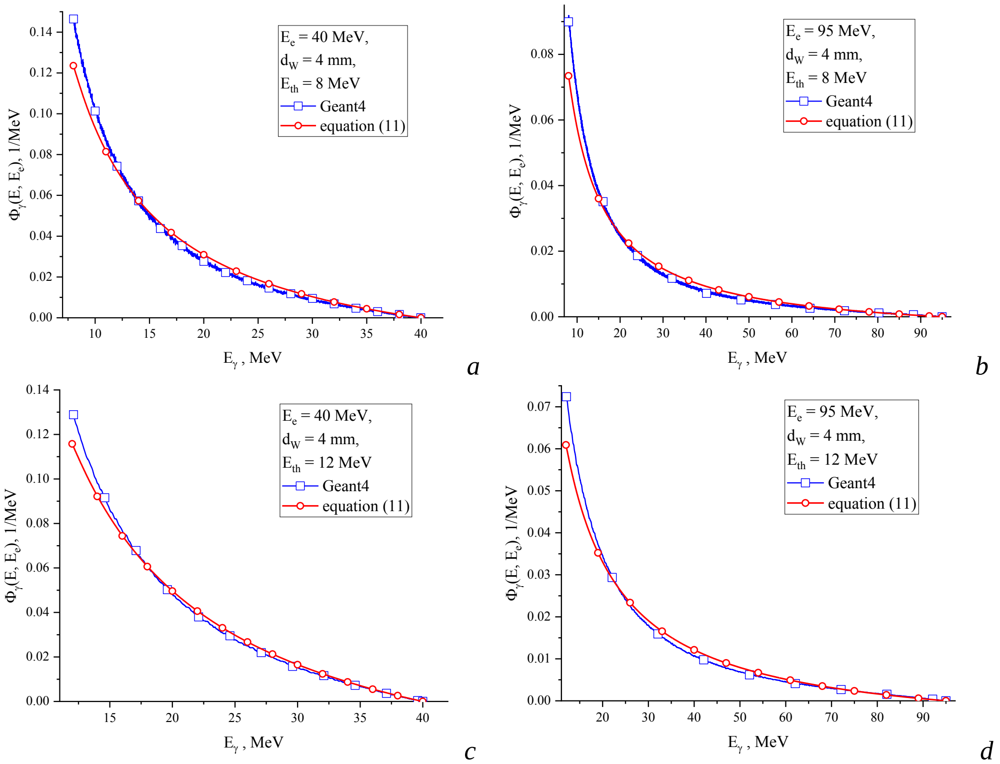


*Fig. 5. Above-threshold photon spectra normalized to one photon*

Comparison of data in Figs. 4 and 5 shows that Eq. (13) describes a spectrum with its normalization to one photon more accurately than that normalized to one electron. This can be explained by subtracting the errors included in the numerator and denominator of the Eq. (13). For the additional verification of accuracy of the Eq. (11), we calculated on its basis the averaged over the photon flux cross section of the $^{100}Mo(\gamma,n)^{99}Mo$ reaction with well-studied excitation function [15, 18].

***Table 4***

*Flux-averaged cross-section of the $^{100}Mo(\gamma, n)^{99}Mo$ reaction (mb)*

| $E_e$, MeV | *S*-model | MC simulation |
|---|---|---|
| 30 | 55.6 | 55.4 |
| 40 | 48.1 | 48.7 |
| 60 | 39.2 | 40.6 |
| 80 | 34.3 | 36.3 |
| 100 | 31.0 | 33.5 |

For comparison, Table 4 lists also the results obtained using Eq. (10) with spectrum of the bremsstrahlung photons calculated by MC technique. Comparison of data shows that they not differ by more than 8%.

## CONCLUSIONS

The characteristics of a beam of the high-energy bremsstrahlung photons and of the photonuclear processes under its influence can be calculated within an analytical approach based on the three key phenomenological parameters – the photonuclear conversion coefficient, the standard deviation of the radial distribution of the above-threshold photon flux density at the rear surface of the converter and the most probable angle of their escape.

The conditions under which these parameters can be measured in the experiment are shown. The minimum width of the electron beam at the input of the bremsstrahlung converter, which ensures the Gaussian distribution of the photon flux density as well as an explicit form of its profile dependence on primary beam and converter characteristics have been established.

To unify the conditions of the photonuclear measurements, in particular, determination of reaction cross section averaged over the photon flux on the target, it is expedient to activate the latter in the photonuclear converter mode at a photon spectrum integrated over exit angle. A phenomenological representation is proposed and verified for such a spectrum depended only on the reaction threshold and photon end-point energy. Its reproduction in the range of 40…100 MeV can be ensured with high accuracy using a Ta or W converter by 3…4 mm in thickness.

## REFERENCES


1. K. Devan, A.K.M.M.H. Meaze, Guinyun Kim, et al. Photo-Neutrons Produced, at the Pohang Neutron Facility Based on an Electron Linac // *J. of Korean Phys. Soc*. 2006, v. 49, № 1, p. 89-96.
2. Yo. Gohar, L.L. Briggs, Ya. Cao, et al. *Neutron Source Facility of the National Science Center “Kharkiv Institute of Physics and Technology” at Kharkiv, Ukraine*. United States: N. Web. doi:10.2172/1900255 (2022).
3. X.L. Wang, Z.Y. Xu, W. Luo, et al. Transmutation prospect of long-lived nuclear waste induced by high-charge electron beam from laser plasma accelerator. 2017. https://arxiv.org/ftp/arxiv/papers/1705/1705.05770.pdf.
4. D.J.S. Findlay. Application of phononuclear reactions //*Nucl. Instr. and Meth*. 1990, v. B50, p. 314-320.
5. S. Segebade, H.-P Weise, G.J. Lutz. *Photon Activation Analysis*. New York, Hawthorhe, 1987, 705 p.
6. M.P. Dykiy, A.N. Dovbnya Yu.V. Lyashko, et al. Photonuclear production of $^{193m,195m}$Pt and synthesis of radioactive cisplatin // *J. Labell. Comp. Radiopharm*. 2007, v. 50, p. 480-482.
7. V.I. Nikiforov and V.L. Uvarov. Development of the technique embedded into a Monte Carlo transport system for calculation of photonuclear isotope yield // *Nukleonika.* 2012, v. 57, p. 75-80 (in Russian).
8. V.L. Uvarov, A.A. Zakharchenko, N.P. Dikiy, et al. Development and validation of an analytical model of isotope production by bremsstrahlung radiation // *Appl. Rad. and Isot.* 2023, v. 199, p. 110890.
9. D.J.S. Findlay. Analytic representation of bremsstrahlung spectra from thick radiators as a function of photon energy and angle // *Nucl. Instr. and Meth*. 1989, v. A276, p. 598-601.
10. H. Utsunomiya, I. Gheorghe, D.M. Filipescu, et al. GDR cross sections updated in the IAEA-CRP // *Proc. of EPJ Web Conf. ND 2019: International Conference on Nuclear Data for Science and Technology*. 2020, v. 239, 01002, 6 p.
11. V.D. Napoli, A.M. Lacerenza, F. Salvetti, et al. Production of $^{24}$Na and $^{22}$Na from $^{27}$Al by high-energy photons // *Lett. Nuovo Cimento.* 1971, № 1, p. 835-838**.**
12. J. Allison, K. Amako, J. Apostolakis, et al. Recent developments in Geant4 // *Nucl. Instr .and Meth.* 2016, A835, p. 186-225.
13. M.I. Aizatskyi, V.I. Beloglasov, V.N. Boriskin, et al. State and Prospects of the Linac of Nuclear-Physics Complex with Energy of Electrons up to 100 MeV // *Problems of Atomic Science and Technology. Series “Nuclear Physics Investigations”*. 2014, № 3, p. 60-63.
14. Evaluated Nuclear Data File ENDF/B-VIII.0, Brookhaven National Laboratory. 2018. ENDF/B-VIII. https://www.nndc.bnl.gov/endf/.
15. TALYS-1.95, https://tendl.web.psi.ch/tendl_2019/talys.html.
16. T.R. Sherwood, W.E. Turchinetz. Some photodisintegration reactions in the titanium isotopes // *Nuclear Physics*. 1962, v. 29, p. 292-295.
17. N.P. Dikiy, Yu.V. Lyashko, V.A. Shevchenko, et al. An Estimate of $^{47}$Sc Photonuclear Yield in a Production Target // *Problems of Atomic Science and Technology. Series “Nuclear Physics Investigations”*. 2020, № 3, p. 158-162.
18. Experimental Nuclear Reaction Data Base (EXFOR), NNDC, Brookhaven National Laboratory, 2014. https://www-nds.iaea.org/exfor.


*Article received 21.09.2023*

## ФОРМУВАННЯ ТА ФЕНОМЕНОЛОГІЧНИЙ ОПИС ПУЧКА ГАЛЬМІВНОГО ВИПРОМІНЮВАННЯ ДЛЯ ФОТОЯДЕРНИХ ПРОЦЕСІВ

***В.Л. Уваров, О.О. Захарченко, М.П. Дикий, Ю.В. Ляшко, Р.І. Помацалюк, В.А. Шевченко, Є.Б. Малець***

У рамках розробленої аналітичної моделі для опису напрацювання ізотопів гальмівним випромінюванням встановлено три ключові феноменологічні параметри процесу. Ці параметри визначають загальний вихід та об'ємний розподіл у мішені продуктів фотоядерної реакції з домінуванням гігантського дипольного резонансу (ГДР). Досліджуються умови застосування та точність феноменологічного опису характеристик потоку понадпорогових гальмівних фотонів. Запропоновано форму опису референтного спектра гальмівного випромінювання для аналітичного розрахунку фотоядерних процесів. Досліджено умови та точність його відтворення в експерименті.